Journal of the European Ceramic Society 18 (1998) 907–914

PII: S0955-2219(97)00180-5
0955-2219/98/$19.00 + 0.00

Microstructure and High-Temperature Strength of Si_3N_4–SiC Nanocomposite

Hyoungjoon Park,[a] Hyoun-Ee Kim[a,*] and Koichi Niihara[b]

[a]Department of Inorganic Materials Engineering, Seoul National University, Seoul, 151-742, Korea
[b]I.S.I.R., Osaka University, 8-1 Mihogaoka, Ibaraki-shi, 567 Osaka, Japan

(Received 11 June 1997; accepted 11 August 1997)

Abstract

The microstructural evolution and the high-temperature strength of Si_3N_4–SiC nanocomposite hot pressed with Yb_2O_3 as a sintering aid were investigated. The microstructure of the composite was influenced by the nucleation step prior to the densification. When the number of nucleation sites was small, large elongated grains were formed and large fraction of the SiC particles was trapped inside the grains. On the other hand, when there were many nucleation sites, the grains became small because of the inhibition of growth of β-Si_3N_4 grains by the SiC particles, and most of the SiC particles were located on the grain boundaries. The number of nucleation site was controlled by the heat treatment temperature before the densification. The location of the SiC particles was important in determining the high-temperature strength of this composite material. The strength was improved only when the SiC particles were located on the grain boundaries. The flexural strength of Si_3N_4 with 20 vol% SiC was 1150 ± 50 MPa at room temperature. The strength was maintained at elevated temperatures up to 1200°C and decreased to 1000 MPa at 1400°C in air.

1 Introduction

Silicon nitride (Si_3N_4) is one of the most promising ceramic materials for high-temperature structural applications because of its excellent thermomechanical properties. However, being a covalent material Si_3N_4 should be sintered with appreciable amount of oxide additives. During densification these additives react with the Si_3N_4 particles, forming an eutectic liquid which results in amorphous phases at the grain boundaries upon cooling. It is these amorphous phases that soften at temperatures above ~1000°C, causing grain-boundary sliding and an eventual failure of the material.[1–3] Therefore, to obtain a Si_3N_4 useful at elevated temperatures, it is necessary to enhance the refractoriness of the grain boundary phase.

Much effort has been made to select an oxide additive which is suitable for the densification of Si_3N_4 and at the same time has high refractoriness as a boundary phase.[4–9] Crystallization of the boundary phase by heat treatment after the densification is another viable method to improve the refractoriness of the boundary phase.[10–13] Most rare-earth oxides satisfied these two conditions, i.e. the grain boundary phases formed by using the rare-earth oxides as sintering aids have relatively high refractoriness and the refractoriness is further improved by the crystallization of the phases after the densification.[14–17] The crystallization of the boundary phases, however, sometimes acted adversely on other mechanical properties such as fracture toughness and room-temperature strength of the Si_3N_4.[14,18]

Another method to increase the high-temperature strength of Si_3N_4 is to disperse crystalline particles with high refractoriness at the grain boundaries. The high-temperature strength was improved when the grain-boundary sliding is effectively inhibited by the particles.[19,20] However, this approach should be employed with caution because of the possibility of formation of microcracks around the particles due to thermal expansion mismatches.[19] To minimize the formation of microcracks very fine particles should be used as a second phase.

Recently, ceramic/ceramic nanocomposites, in which nanometer-size second phase was dispersed in the matrix grains, were successfully fabricated. The dispersion of fine (100 to 300 nm) particles in matrices of higher thermal expansion coefficient increased the strength of the materials significantly.

*To whom correspondence should be addressed.

For example, the strengths of alumina and magnesia were improved remarkably by the addition of small amounts (~5 vol%) of fine SiC particles.[21–25] The strengthening was attributed by many researchers to the reduction of average grain size,[21,22] surface compressive stress induced by machining,[25] crack deflection due to residual stress,[26,27] and crack healing and residual stress relaxation during annealing.[28–30]

The Si_3N_4–SiC nanocomposites were also fabricated by hot pressing either the amorphous Si–C–N precursor powders prepared by a CVD process or the mixtures of Si_3N_4 and SiC powders with Y_2O_3/Al_2O_3 as a sintering aid.[31–33] Increases in the strength and the fracture toughness were observed from the composites compared to the monolithic Si_3N_4. Different from the Al_2O_3–SiC nanocomposites, however, the increases in strength were mainly due to the changes in microstructure. The high-temperature strength and the slow crack resistance were also improved by making the nanocomposite. The increase in high-temperature strength was presumed to be due to either the thermal expansion mismatch or the modification of the interface structure.[34–37]

We previously observed that when Yb_2O_3 was used as a sintering aid, the high-temperature strength of Si_3N_4 was improved significantly due to the formation of crystalline $Yb_4Si_2O_7N_2$ at the grain boundaries.[38] It is of interest to examine whether the dispersion of fine refractory particles at the grain boundaries further increases the high-temperature strength of the Si_3N_4. In the present study, we investigated the role of nano-sized SiC particles on the microstructural evolution and the high-temperature strength of Si_3N_4 hot-pressed with Yb_2O_3 as a sintering aid. The effect of nucleation process before the densification on the final microstructure was also investigated and related to the high-temperature flexural strength of the material.

2 Experimental Procedure

Si_3N_4 powder (SN E-10, Ube Industries, Tokyo, Japan) with high specific surface area ($11{\cdot}5\,m^2\,g^{-1}$) and high $\alpha/(\alpha+\beta)$ ratio (over 95%) was used as a starting material, and high purity Yb_2O_3 (99·99%, High Purity Chemical Co. Tokyo, Japan) was used as a sintering aid. Various amounts (0 to 20 vol%) of nanosize β-SiC powder with average particle size of $0{\cdot}3\,\mu m$ (UF grade, Ibiden Co., Ltd., Tokyo, Japan) were used as a dispersoid. The amount of Yb_2O_3 addition was fixed to 14 wt%. The powders were mixed by ball milling in ethanol for 24 h with silicon nitride balls as media. Weights of the milling media and the container measured before and after the milling showed contamination by the ball or the container was negligible. After the mixed slurry was dried in a rotation evaporator, it was dry ball milled again for 6 h to crush the soft agglomerates. The powder mixtures were hot-pressed in a graphite die of diameter 44 mm at 1800°C for 2 h after being kept at various temperatures (1400–1600°C) for 3 h for the nucleation of β-grains. The hot-pressing was carried out in flowing N_2 atmosphere with the applied pressure of 30 MPa. The cooling rate was $20°C\,min^{-1}$ down to 800°C and furnace cooling thereafter. Bulk densities were measured by the Archimedes method.

Microstructures of the hot-pressed specimens were observed with an SEM after etching the polished surface with NaOH at 500°C for 9 s. Some of the specimens were crushed into powders to determine the grain boundary phases and the α–β transformation rate of Si_3N_4 using an X-ray diffractormeter (Ru-200B, Regaku Co. Ltd., Japan). Grain boundary phases, nucleation process and the location of SiC particles were also examined with a transmission electron microscope (H-8100, Hitachi Co. Ltd., Japan). Specimens for TEM were prepared by mechanical thinning and subsequently by ion milling to achieve electron transparency. A thin layer of gold or carbon was deposited on the surfaces of SEM and TEM specimens to avoid electron beam charging.

Flexural strengths were measured at room- and elevated-temperatures up to 1400°C in air with a crosshead speed of $0.5\,mm\,min^{-1}$ by three-point bend test with outer span of 30 mm. Test specimens with dimension of 3×4×40 mm were cut and machined from the hot-pressed disks. Three-point bend test was employed for its convenience to measure the high-temperature strength. All the specimens were ground up to 800-grit diamond wheel and tensile surfaces were polished with diamond slurries up to 0·5 micron. Edges were chamfered to eliminate machining flaws that could act as fracture origins. For the high-temperature bending test, a box furnace was placed between frames of a testing instrument (AG-10TC, Shimadzu Co. Ltd., Japan). The heating rate was $10°C\,min^{-1}$ and after reaching the test temperature, the temperature was maintained for an additional 10 min prior to testing for thermal stability. At least five specimens were tested for each set of conditions.

3 Results and Discussion

3.1 Effect of SiC content

All the specimens hot-pressed at 1800°C with various amounts of SiC had higher than 99% of

theoretical density. The effect of SiC content on the microstructural evolution of Si_3N_4 is shown in Fig. 1. When no SiC was added, a microstructure consisting of large elongated grains in fine matrix grains was observed as shown in Fig. 1(A), which is a typical microstructure for monolithic Si_3N_4.[4,6,38] With addition of 5 vol% SiC, the grain size became slightly smaller, as seen in Fig. 1(B). This micrograph also illustrates that some of the SiC particles were located inside the elongated grains. When 20 vol% SiC was added, the size of elongated grains became smaller only slightly again, however, the number of SiC particles inside the large grains became much higher as seen in Fig. 1(C). These micrographs show that the morphology of Si_3N_4 was not much changed by the addition of the SiC nanoparticles.

The grain boundary composition was also not much affected by the SiC particles. X-ray diffraction patterns of the Si_3N_4 with different amounts of SiC are shown in Fig. 2. When no SiC was added, the grain boundary phase was identified as a crystalline $Yb_4Si_2O_7N_2$. According to previous selected-area diffraction pattern analyses,[38] this crystalline phase was found in large triple pockets, while an amorphous phase was detected in small triple pockets and two grain junctions. With additions of 5 and 20 vol% of SiC, the composition of the boundary phase was not changed, however, the increases in intensity of boundary phase (crystalline $Yb_4Si_2O_7N_2$) as well as that of SiC were seen clearly in Fig. 2(B) and (C), respectively. The formation of crystalline $Yb_4Si_2O_7N_2$ at the triple pockets of the specimen with 20 vol% SiC was confirmed by the selected-area diffraction pattern as seen in Fig. 3.

The strengths of the Si_3N_4–SiC nanocomposite material containing 20 vol% SiC at various temperatures are shown in Fig. 4, along with those of monolithic Si_3N_4. As seen in this graph, the strength of Si_3N_4 remained basically same by the addition of SiC particles both at room and at elevated temperatures. This result implied that the increase in the grain-boundary crystalline phase or the reduction in grain size were not significant enough to influence the strength of the composite material. Effect of residual stress due to thermal expansion mismatch was also expected to be negligible, especially at elevated temperatures, because of small difference in the thermal expansion coefficient of Si_3N_4 ($3{\cdot}5\times10^{-6}$ K^{-1}) and that of SiC ($4{\cdot}5\times10^{-6}$ K^{-1}).

Based on these results, it is clear that to increase the high-temperature strength of Si_3N_4, the microstructure of the composite should be modified. Ideal microstructure for this purpose is one in which the SiC particles are uniformly dispersed at

Fig. 1. SEM micrographs of Si_3N_4 containing (A) 0 vol%, (B) 5 vol%, and (C) 20 vol% of SiC nanoparticles. All the specimens were hot-pressed with 14 wt% of Yb_2O_3 at 1800°C for 2 h.

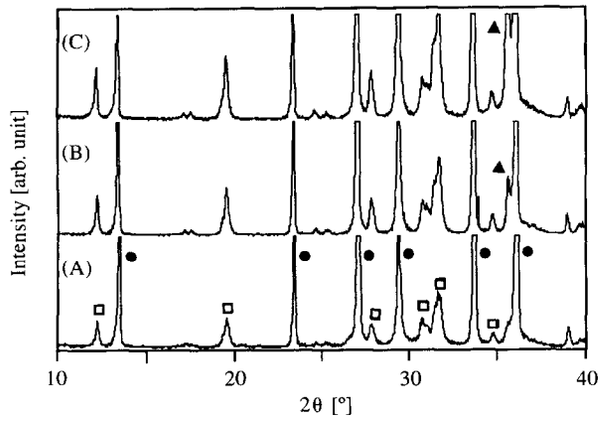

Fig. 2. X-ray diffraction patterns of hot-pressed Si_3N_4 containing (A) 0 vol%, (B) 5 vol%, and (C) 20 vol% of SiC nanoparticles. ●, β-Si_3N_4; □, $Yb_4Si_2O_7N_2$; ▲, SiC.

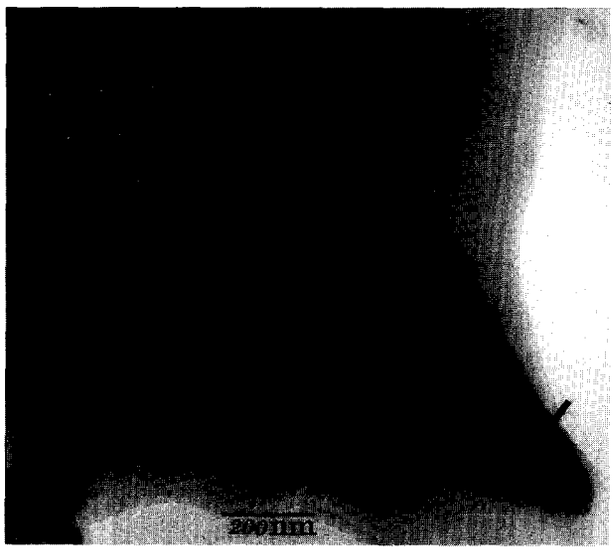

Fig. 3. TEM micrograph on the grain boundary region of the specimen containing 20 vol% SiC nanoparticles. Electron diffraction pattern shows that the grain boundary is mainly composed of crystalline $Yb_4Si_2O_7N_2$.

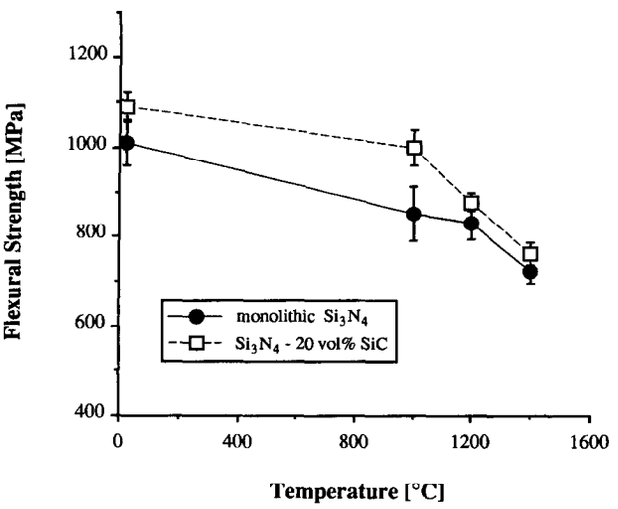

Fig. 4. Strengths of Si_3N_4–SiC nanocomposite containing 20 vol% SiC compared to those of monolithic Si_3N_4 at various temperatures.

the grain boundaries, effectively inhibiting the grain boundary sliding at elevated temperatures.[9,19,23] The microstructure of the Si_3N_4–SiC composite was optimized by controlling the nucleation step before the densification.

3.2 Effect of nucleation step

When the SiC particles are added to the Si_3N_4, there are two possibilities about the role of the particles on the microstructural evolution of the Si_3N_4.[32–36] First, the SiC may act as nucleation sites for the β-Si_3N_4 grains. In this case, all the SiC particles would be enclosed in the grains, and the average grain size of Si_3N_4 is expected to be reduced as a result of the increase in the number of the nucleation sites. Another possibility is that the SiC may act as a grain growth inhibitor. The dissolution-reprecipitation process and the grain boundary migration of Si_3N_4 are likely to be hindered by the presence of the inert SiC particles. This inhibition effect is proportional to the relative size of the SiC particles and the Si_3N_4 grains. When the size of SiC is much smaller than that of Si_3N_4 grains, the grain growth of Si_3N_4 occurs around the SiC particles easily, trapping the SiC particles inside the Si_3N_4 grains. On the other hand, if the size of the SiC is comparable to that of Si_3N_4 grains, the inhibition effect is expected to be strong, resulting in the reduction of average grain size and leaving the SiC particles at the grain boundaries.[33,36]

TEM observations on the nanocomposite with 20 vol% SiC revealed that most of the small SiC particles ($< 0{\cdot}3\,\mu m$) were trapped inside the Si_3N_4 grains, while the larger ones were located at the grain boundaries, as shown in Fig. 5(A) and (B), respectively. These micrographs implied the decreases in the grain size observed were due to the inhibition of the grain growth of Si_3N_4 by the SiC particles.[37] This inhibition effect was also observed in Al_2O_3–SiC system by Stearns and Harmer recently.[39,40] The effect of SiC content on the amount of β-Si_3N_4 phase after heat treating at 1650°C for 30 min, shown in Fig. 6, supported this premise. The amount of β-phase decreased with the SiC content, suggesting the growth of β-grains after nucleation was inhibited by the SiC particles.

Because of this inhibition effect, the number of nucleation sites for β-Si_3N_4 was critical for the final microstructure. The number was determined by the heat treatment temperature for nucleation (1400–1600°C) before reaching the densification temperature. Figure 7 shows typical TEM images of Si_3N_4 with 20 vol% SiC, heat treated at 1400, 1500 and 1600°C for 3 h before the densification. When heat treated for nucleation at 1400°C, small number of very fine nuclei was formed as shown in Fig. 7(A).

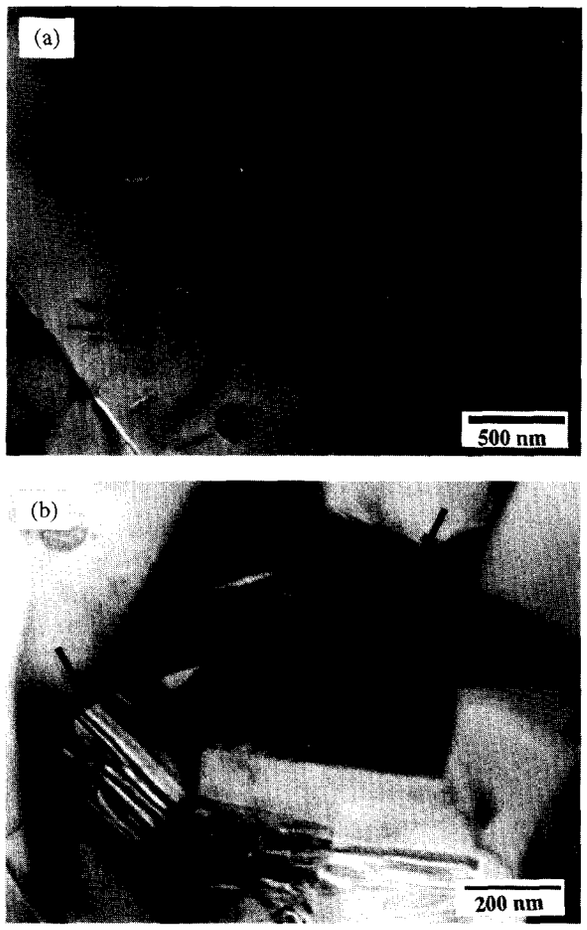

Fig. 5. TEM micrographs of the specimen containing 20 vol% of SiC nanoparticles showing (A) small SiC particles trapped inside the Si_3N_4 grains and (B) large particles located at the grain boundaries.

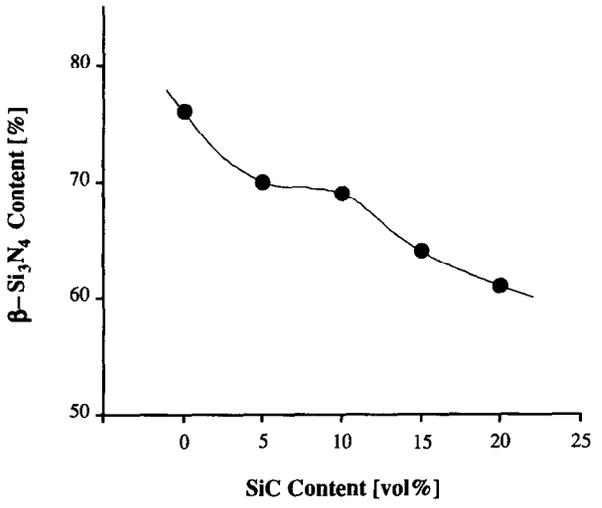

Fig. 6. Effect of SiC contents on the amount of β-Si_3N_4 phase after heat treatment at 1650°C for 30 min. The amount of β-phase decreased with the SiC content, implying the growth of β-grains after nucleation was inhibited by the SiC particles.

As the heat treatment temperature was increased to 1500°C, large number of nuclei with size about 500 nm was observed as shown in Fig. 7(B). When the heat treatment temperature was increased further to 1600°C, large β-Si_3N_4 grains of about 2 μm

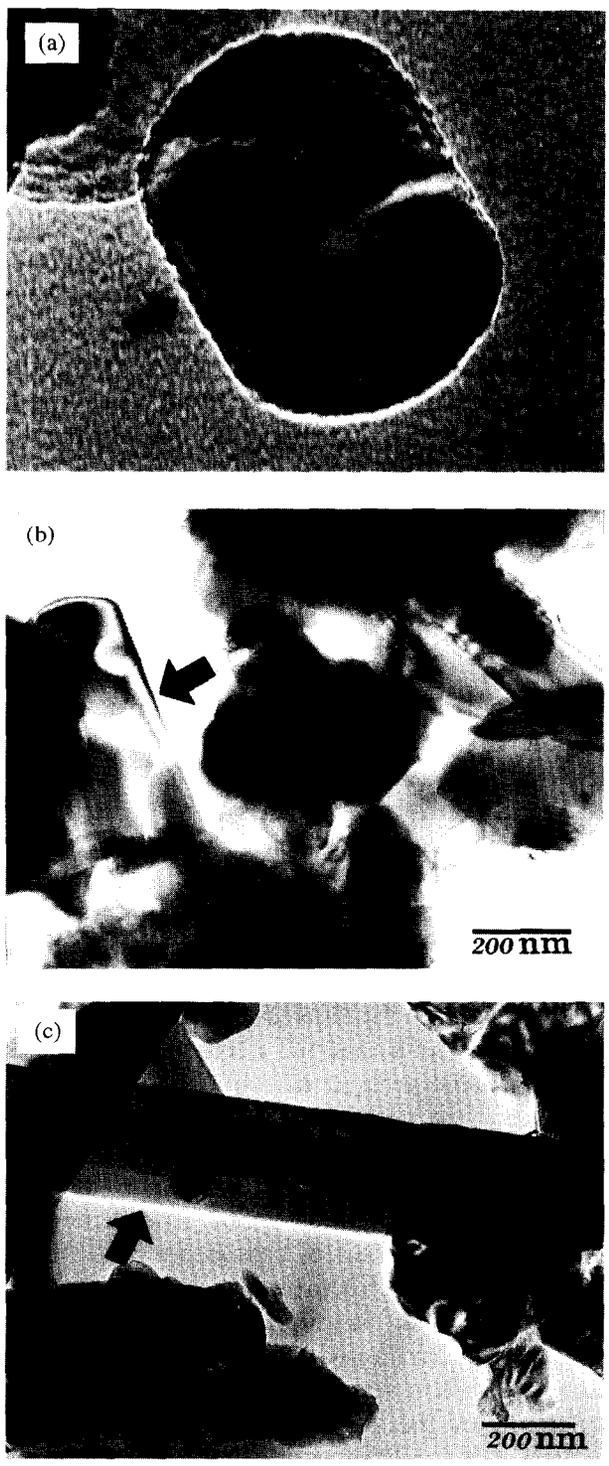

Fig. 7. TEM micrographs of specimens heat treated at (A) 1400, (B) 1500, and (C) 1600°C for 3 h, showing the effect of heat treatment on the size of β-grain nuclei.

were formed as shown in Fig. 7(C), implying an extensive growth of the nuclei at this temperature. These micrographs illustrated that 1500°C was the most appropriate temperature for the nucleation of large number of β-grains without extensive growth.

The final microstructure of the specimen was influenced by these nucleation behaviors. The specimen hot pressed at 1800°C following the heat treatment at 1400°C had a microstructure consisting of large elongated grains and fine matrix,

Fig. 8(A), as a result of fast growth of small number of β-nuclei. As seen in this micrograph, lots of SiC particles were trapped in the large grains. When the heat treatment temperature was increased to 1500°C, the average size of the grains became remarkably smaller, as shown in Fig. 8(B), apparently due to the combined effect of the formation of many β-nuclei during the heat treatment and the inhibition of grain growth by the SiC particles. This micrograph also showed that not many SiC particles were trapped inside the Si_3N_4 grains. Therefore, even though a quantitative analysis on the location of SiC particles was impossible because of the loss of SiC at the grain boundaries during chemical etching, most of the SiC particles were expected to be located on the grain boundaries. These results agreed well with the recent findings by Stearns and Harmer.[39,40] According to their analyses on the grain growth of Al_2O_3–SiC system, the grain-growth rate of Al_2O_3 was reduced remarkably by the SiC particles and the fraction of SiC particles on grain boundaries increased as the average grain size of Al_2O_3 decreased. With further increase in the heat treatment temperature to 1600°C, a microstructure similar to that obtained after heat treatment at 1400°C (i.e. large elongated grains in a fine matrix) was observed as shown in Fig. 8(C). This microstructure is formed by the growth of small number of relatively large β-grains shown in Fig. 7(C). It is interesting to note that the microstructures of the specimens heat treated at 1400 or 1600°C were about the same as that of Si_3N_4 without the heat treatment [Fig. 1(C)].

These variations in microstructure had significant effects on the high-temperature strength of the material. The effect of heat treatment temperature on the high-temperature strength is shown in Fig. 9. As seen in this graph, the high-temperature strength is maximum when the specimen was densified after heat treatment at 1500°C for the nucleation of the β-grains. The improvement in strength was apparently due to the SiC particles located at the grain boundary area, which improved the refractoriness of the grain boundary phase by effectively resisting against the grain boundary sliding.

When Yb_2O_3 was used as a sintering aid of Si_3N_4, excellent high-temperature strength was obtained as a result of the formation of crystalline $Yb_4Si_2O_7N_2$ at the grain boundaries.[9,17,38] The strength was improved further by the addition of the SiC particles. The strength of the composites containing different amounts of SiC nanoparticles at elevated temperatures are shown in Fig. 10. All the specimens were hot pressed after heat treatment at 1500°C for 3 h for the nucleation of the

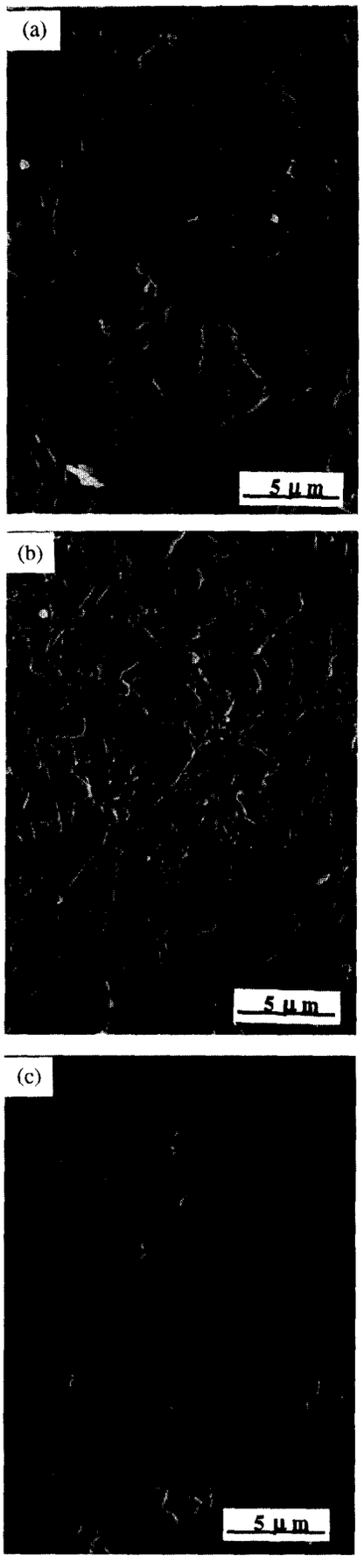

Fig. 8. SEM micrographs of the specimens hot-pressed at 1800°C for 2 h following the heat treatment at (A) 1400, (B) 1500°, and (C) 1600°C for 3 h, showing the variations in the average grain size and the location of SiC particles depending on the heat treatment temperature.

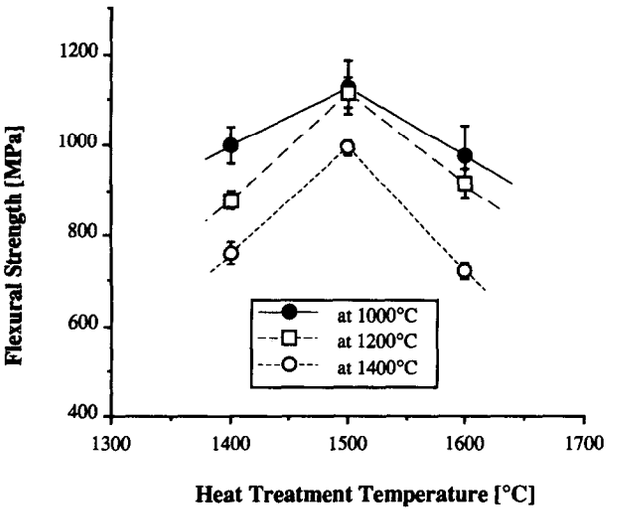

Fig. 9. High-temperature strength of Si_3N_4–SiC nanocomposite containing same amount of SiC (20 vol%) and hot-pressed at same conditions, but heat treated for nucleation at different temperatures. The high-temperature strength was improved only when the SiC particles were located at the grain boundaries.

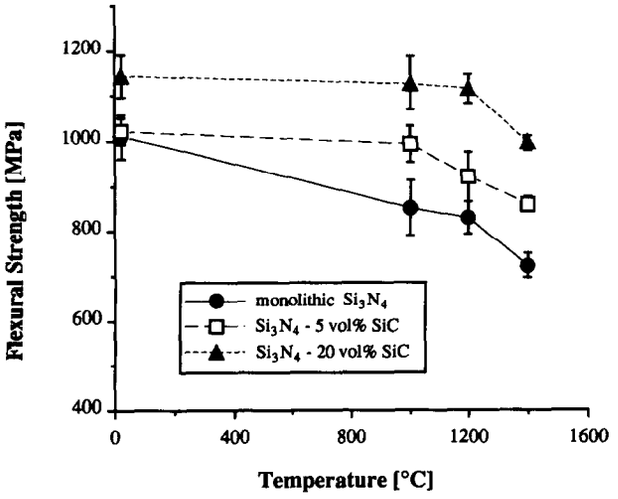

Fig. 10. Flexural strengths of Si_3N_4–SiC nanocomposite containing different amounts of SiC at elevated temperatures. The high-temperature strength of Si_3N_4 was improved significantly by adding 20 vol% SiC nanoparticles.

β-grains. The microstructure and strength of the Si_3N_4 without the SiC were not influenced by such heat treatment. As seen in Fig. 10, the high temperature strength of Si_3N_4 was remarkably improved by the addition of 20 vol% of SiC nanoparticles. This results well exemplified, when compared to the strength in Fig. 4, the importance of the microstructure of a material for the mechanical properties of it.

4 Summary and Conclusions

The microstructural evolution and the high-temperature strength of the Si_3N_4–SiC nanocomposite were investigated. The microstructure of the composite was strongly influenced by the nucleation step before the densification. When the number of the nucleation sites was small, large elongated grains were formed and large fraction of the SiC particles was trapped inside the grains. On the other hand, when there were many nucleation sites, the grains became small because of the inhibition of growth of β-Si_3N_4 grains by the SiC particles and most of the SiC particles were located at the grain boundaries. The location of the SiC particles was important in determining the high-temperature strength of this composite material. The high-temperature strength was improved only when the SiC particles were located at the grain boundaries. When 20 vol% SiC was added, the strength of about 1000 MPa was observed at 1400°C in air. The role of SiC particles is believed to alleviate the softening of the oxide phases at the grain boundaries.

Acknowledgements

Research sponsored by Korean Ministry of Education Research Fund for Advanced Materials in 1996 and by the Korea Science and Engineering Foundation (KOSEF) through the Center for Interface Science and Engineering of Materials as Korea Advanced Institute of Science and Technology (KAIST).

References

1. Sanders, W. A. and Groseclose, L. E., Flexural stress rupture and creep of selected commercial silicon nitrides. *J. Am. Ceram. Soc.*, 1993, **76**, 553–556.
2. Knickerbocker, S. H., Zangvil, A. and Brown, S. D., High-temperature mechanical properties and microstructures for hot-pressed silicon nitrides with amorphous and crystalline intergranular phases. *J. Am. Ceram. Soc.*, 1985, **68**, C99–C101.
3. Tanaka, I., Pezzotti, G., Okamoto, T., Miyamoto, Y. and Koizumi, M., Hot isostatic press sintering and properties of silicon nitride without additives. *J. Am. Ceram. Soc.*, 1989, **72**, 1656–1660.
4. Pyzik, A. J. and Beaman, D. R., Microstructure and properties of self-reinforced silicon nitride. *J. Am. Ceram. Soc.*, 1993, **76**, 2737–2744.
5. Sanders, W. A. and Mieskowski, D. M., Strength and microstructure of sintered Si_3N_4 with rare-earth-oxide additions. *Am. Ceram. Soc. Bull.*, 1985, **64**, 304–309.
6. Mazdiyasni, K. S. and Cooke, C. M., Consolidation, microstructure, and mechanical properties of Si_3N_4 doped with rare-earth oxides. *J. Am. Ceram. Soc.*, 1974, **57**, 536–537.
7. Wang, C.-M., Pan, X., Hoffmann, M. J., Cannon, R. M. and Ruhle, M., Grain boundary films in rare-earth-glass-based silicon nitride. *J. Am. Ceram. Soc.*, 1996, **79**, 788–792.
8. Cinibulk, M. K., Thomas, G. and Johnson, S. M., Strength and creep behavior of rare-earth disilicate-silicon nitride ceramics. *J. Am. Ceram. Soc.*, 1195, **75**, 2050–2055.
9. Hoffmann, M. J., High-temperature properties of Si_3N_4 ceramics. *MRS Bull.*, 1995, **xx**, 28–32.

10. Weston, J. E. and Pratt, P. L., Crystallization of grain boundary phases in hot-pressed silicon nitride materials. *J. Mater. Sci.*, 1978, **13**, 2147–2156.
11. Pierce, L. A., Mieskowski, D. M. and Sanders, W. A., Effect of grain-boundary crystallization on the high-temperature strength of silicon nitride. *J. Mater. Sci.*, 1986, **21**, 1345–1348.
12. Bonnell, D. A., Tien, T.-Y. and Ruhle, M., Controlled crystallization of the amorphous phase in silicon nitride ceramics. *J. Am. Ceram. Soc.*, 1987, **70**, 460–465.
13. Cinibulk, M. K., Thomas, G. and Johnson, S. M., Fabrication and secondary-phase crystallization of rare-earth disilicate–silicon nitride ceramics. *J. Am. Ceram. Soc.*, 1992, **75**, 2037–2043.
14. Cinibulk, M. K., Thomas, G. and Johnson, S. M., Grain-boundary-phase crystallization and strength of silicon nitride sintered with YSiAlON glass. *J. Am. Ceram. Soc.*, 1990, **73**, 1606–1612.
15. Tsuge, A., Nishida, K. and Komatsu, M., Effect of crystallizing the grain–boundary glass phase on the high-temperature strength of hot-pressed Si_3N_4 containing Y_2O_3. *J. Am. Ceram. Soc.*, 1975, **58**, 323–326.
16. Clarke, D. R., Lange, F. F. and Schnittgrund, G. D., Strengthening of a sintered silicon nitride by a post-fabrication heat treatment. *J. Am. Ceram. Soc.*, 1982, **65**, C51–C53.
17. Hoffmann, M. J., High-temperature properties of Yb-containing Si_3N_4. In *Tailoring of Mechanical Properties of Si_3N_4 Ceramics*, ed. M. J. Hoffmann and G. Petzow. 1993, Kluwer, Dordrecht, pp. 233–244.
18. Peterson, I. M. and Tien, T.-Y., Effect of the grain boundary thermal expansion coefficient on the fracture toughness in silicon nitride. *J. Am. Ceram. Soc.*, 1995, **78**, 2345–2352.
19. Lange, F. F., Effect of microstructure on strength of Si_3N_4–SiC composite system. *J. Am. Ceram. Soc.*, 1973, **56**, 445–450.
20. Ohji, T., Nakahira, A., Hirano, T. and Niihara, K., Tensile creep behavior of alumina/silicon carbide nanocomposite. *J. Am. Ceram. Soc.*, 1994, **77**, 3259–3262.
21. Niihara, K. and Nakahira, A., Strengthening of oxide ceramics by SiC and Si_3N_4 dispersions, In *Proceedings of the Third International Symposium on Ceramic Materials and Components for Engines*. The American Ceramic Society, Westerville, OH, 1988, pp. 919–926.
22. Niihara, K., Nakahira, A., Sasaki, G. and Hirabayashi, M., Development of strong Al_2O_3 composites. In *Proceedings of the International Meeting on Advanced Materials*, Vol. 4. The Materials Society of Japan, Kawasaki, Japan, 1989, pp. 124–134.
23. Yasuda, E., Bao, Q., Tanabe, Y. and Niihara, K., High temperature creep of SiC/MgO nanocomposite. In Proceedings of the 1st International Symposium on Science of Engineering Ceramics, 1989, The Ceramic Society of Japan, Koda, pp. 431–436.
24. Stearns, L. C., Zhao, J. and Harmer, M. P., Processing and microstructure development in Al_2O_3–SiC nanocomposite. *J. Eur. Ceram. Soc.*, 1992, **10**, 473–477.
25. Zhao, J., Stearns, L. C., Harmer, M. P., Chan, H. M., Miller, G. A. and Cook, R. F., Mechanical behavior of alumina-silicon carbide nanocomposite. *J. Am. Ceram. Soc.*, 1993, **76**, 503–510.
26. Levin, I., Kaplan, W. D., Brandon, D. G. and Layyous, A. A., Effect of SiC submicrometer particle size and content on fracture toughness of alumina-SiC nanocomposites. *J . Am. Ceram. Soc.*, 1995, **78**, 254–256.
27. Levin, I., Kaplan, W. D., Brandon, D. G. and Wieder, T., Residual stresses in alumina–SiC nanocomposites. *Acta. Metall. Mater.*, 1994, **42**, 1147–1154.
28. Thompson, A. M., Chan, H. M., Harmer, M. P. and Cook, R. F., Crack healing and stress relaxation in Al_2O_3–SiC nanocomposite. *J. Am. Ceram. Soc.*, 1995, **78**, 567–571.
29. Fang, J., Chan, H. M. and Harmer, M. P., Residual stress relaxation behavior in Al_2O_3–SiC nanocomposite. *Mater. Sci. & Eng.*, 1995, **A195**, 163–167.
30. Chou, I. A., Chan, H. M. and Harmer, M. P, Machining-induced surface residual stress behavior in Al_2O_3–SiC nanocomposites. *J. Am. Ceram. Soc.*, 1996, **79**, 2403–409.
31. Niihara, K., Hirano, T., Nakahira, A., Ojima, K., Izaki, K. and Kawakami, T., High-temperature performance of Si_3N_4–SiC composites from fine, amorphous Si–C–N powder. In *Proceedings of MRS International Meeting on Advanced Materials*, Vol. 5, Materials Research Society, Tokyo, 1989, pp. 107–112.
32. Sawaguchi, A., Toda, K. and Niihara, K., Mechanical and electrical properties of silicon nitride-silicon carbide nanocomposite material. *J. Am. Ceram. Soc.*, 1991, **74**, 1142–1144.
33. Izaki, K., Nakahira, A. and Niihara, K., Si_3N_4/SiC nanocomposites from amorphous Si–C–N powder precusor. In Proceedings of the 1st International Symposium on Science of Engineering Ceramics. The Ceramic Society of Japan, Koda, 1989, pp. 443–448.
34. Rouxel, T., Wakai, F. and Sakaguchi, S., R-curve behavior and stable crack growth at elevated temperature (1500°–1650°C) in a Si_3N_4/SiC nanocomposite. *J. Am. Ceram. Soc.*, 1994, **77**, 3237–3243.
35. Niihara, K., Suganuma, K., Nakahira, A. and Izaki, K., Interfaces in Si_3N_4–SiC nano-composite. *J. Mater. Sci. Lett.*, 1990, **9**, 598–599.
36. Niihara, K., Izaki, K. and Kawakami, T., Hot-pressed Si_3N_4–32% SiC nanocomposite from amorphous Si–C–N powder with improved strength above 1200°C. *J. Mater. Sci. Lett.*, 1990, **10**, 112–114.
37. Hirano, T. and Niihara, K., Microstructure and mechanical properties of Si_3N_4/SiC composites. *Materials Lett.*, 1995, **22**, 249–254.
38. Park, H., Kim, H.-E. and Niihara, K., Microstructural evolution and mechanical properties of Si_3N_4 with Yb_2O_3 as a sintering additive. *J. Am. Ceram. Soc.*, 1997, **80**, 750–756.
39. Stearns, L. C. and Harmer, M. P., Particle-inhibited grain growth in Al_2O_3–SiC: I, experimental results. *J. Am. Ceram. Soc.*, 1996, **79**, 3013–3019.
40. Stearns, L. C. and Harmer, M. P., Particle-inhibited grain growth in Al_2O_3–SiC: II, equilibrium and kinetic analyses. *J. Am. Ceram. Soc.*, 1996, **79**, 3020–3028.